The Starting Members of the Series $Pr_{4n+2}(C_2)_nBr_{5n+5}$ (n = 1, 2, 3)

Manuel Christian Schaloske[a], Hansjürgen Mattausch[a], Viola Duppel[a], Lorenz Kienle[b], and Arndt Simon[a]

[a] Max Planck Institute for Solid State Research, Heisenbergstraße 1, 70569 Stuttgart, Germany
[b] Technische Fakultät, Institut für Materialwissenschaft, Christian-Albrechts-Universität zu Kiel, Kaiserstraße 2, 24143 Kiel, Germany

Reprint requests to Prof. Dr. Dr. h. c. mult. Arndt Simon. Fax: +49-(711)-689-1091.
E-mail: A.Simon@fkf.mpg.de

Z. Naturforsch. **2009**, *64b,* 922 – 928; received June 4, 2009

The compounds $Pr_6(C_2)Br_{10}$, $Pr_{10}(C_2)_2Br_{15}$ and $Pr_{14}(C_2)_3Br_{20}$ were prepared from $PrBr_3$ and the appropriate amounts of Pr and C and characterized by X-ray structure analyses of single crystals. All three compounds crystallize in space group $P\bar{1}$ with lattice parameters a = 7.571(2), b = 9.004(2), c = 9.062(2) Å, α = 108.57(3), β = 97.77(3), γ = 106.28(3)° for $Pr_6(C_2)Br_{10}$; a = 9.098(2), b = 10.127(2), c = 10.965(2) Å, α = 70.38(3), β = 66.31(3), γ = 70.84(3)° for $Pr_{10}(C_2)_2Br_{15}$; a = 9.054(2), b = 10.935(2), c = 13.352(3) Å, α = 86.27(3), β = 72.57(3), γ = 66.88(3)° for $Pr_{14}(C_2)_3Br_{20}$. They are members of a general series $Ln_{4n+2}(C_2)_nBr_{5n+5}$ and isostructural with the corresponding iodides known for Ln = La, Ce, Pr. $Pr_6(C_2)Br_{10}$ was further characterized *via* transmission electron microscopy techniques.

Key words: Praseodymium, Bromide, Cluster, TEM

Introduction

The early recognized cluster condensation in the unusual structure of NbO [1] turned out to be an ordering principle for a plethora of structures of metal-rich transition metal (M) compounds with p elements (X) [2, 3]. Beside others, especially M_6X_8 and M_6X_{12} clusters occur which are connected *via* the vertices, edges or faces of the M_6 octahedra forming dimers, oligomers and assemblies of higher dimensionality. Moreover this concept proved its value for the exploration of new substance groups, *i. e.* the metal-rich rare-earths halides containing empty or occupied, discrete or condensed clusters [4 – 6].

Regarding the known examples of one-dimensionally linked structures, a homologous series with the general formula $Ln_{4n+2}(C_2)_nX_{5n+5}$ (Ln = lanthanide) has been established [7]. It starts with $Ln_6(C_2)I_{10}$ (Ln = La [8], Ce, Pr [9]) exhibiting isolated Ln_6 octahedra, followed by $Ln_{10}(C_2)_2I_{15}$ (Ln = La [8]) and $Ln_{14}(C_2)_3I_{20}$ (Ln = La, Ce [7, 10], Pr [11, 12]), which contain edge-sharing double and triple octahedra, respectively. An infinite chain of clusters, $Ln_4(C_2)I_5$, is also known for La, Ce and Pr [13].

By now, several different structures based on double-octahedra are known, namely $Gd_{10}(C_2)_2I_{16}$ [14], $Pr_{10}(C_2)_2Br_{16}$ [15], $Gd_{10}(C_2)_2Cl_{17}$, and $Gd_{10}(C_2)_2Cl_{18}$ [16].

In this contribution we describe the preparation and crystal structures of the starting members of the series containing Br as the halogen component. In detail the compounds $Pr_6(C_2)Br_{10}$, $Pr_{10}(C_2)_2Br_{15}$ and $Pr_{14}(C_2)_3Br_{20}$ are presented.

Experimental Section

Synthesis

Praseodymium metal (pieces of 1 – 3 mm edge length, sublimed, 99.99 %, Alfa-Aesar), $PrBr_3$ and graphite powder (pure, Aldrich) were used as starting materials for syntheses. $PrBr_3$ was synthesized from the reaction of Pr_6O_{11} with NH_4Br in aqueous HBr and heated to dryness [17]. The raw product was purified twice by sublimation in a Ta tube at 900 °C / 10^{-4} torr. All handling was carried out under Ar atmosphere either in a glovebox (M. Braun) or through the Schlenk technique.

1.0 g of the mixture of the starting materials was arc-sealed in Ta tubes under Ar atmosphere. Then the Ta tubes were enclosed in silica glass ampoules under vacuum.

The ampoules were annealed for several days at different temperatures and then quenched in water.

$Pr_6(C_2)Br_{10}$: A mixture of Pr : $PrBr_3$: C in a molar ratio of 4 : 5 : 3 was annealed for 17 days at 850 °C. Black polyhe-

Table 1. Crystal data and structure refinement of $Pr_6(C_2)Br_{10}$, $Pr_{10}(C_2)_2Br_{15}$ and $Pr_{14}(C_2)_3Br_{20}$.

Sum formula	$Pr_6(C_2)Br_{10}$	$Pr_{10}(C_2)_2Br_{15}$	$Pr_{14}(C_2)_3Br_{20}$
Formula weight, g mol^{-1}	1668.58	2655.79	3643.00
Color, habitus	black, polyhedral	silver, polyhedral	black, polyhedral
Temperature, K	293(2)	293(2)	293(2)
Wavelength; radiation, Å	AgK_α; 0.56086	MoK_α; 0.71073	MoK_α; 0.71073
Crystal system	triclinic	triclinic	triclinic
Space group	$P\bar{1}$	$P\bar{1}$	$P\bar{1}$
a, Å	7.571(2)	9.098(2)	9.054(2)
b, Å	9.004(2)	10.127(2)	10.935(2)
c, Å	9.062(2)	10.965(2)	13.352(3)
α, deg	108.57(3)	70.38(3)	86.27(3)
β, deg	97.77(3)	66.31(3)	72.57(3)
γ, deg	106.28(3)	70.84(3)	66.88(3)
Volume, Å^3	544.8(2)	849.3(3) Å^3	1157.8(4) Å^3
Formula units per unit cell	1	1	1
Density (calcd.), g cm^{-3}	5.09	5.19	5.23
Absorption coefficient, mm^{-1}	16.8	31.7	31.7
$F(000)$	716	1139	1562
Crystal dimensions, mm^3	$0.24 \times 0.16 \times 0.12$	$0.10 \times 0.08 \times 0.06$	$0.18 \times 0.14 \times 0.12$
Diffractometer	IPDS I (Stoe, Darmstadt)	IPDS II (Stoe, Darmstadt)	IPDS II (Stoe, Darmstadt)
Measured ϑ range	$2.60° \le \vartheta \le 27.50°$	$3.36° \le \vartheta \le 24.99°$	$2.51° \le \vartheta \le 28.50°$
Index ranges	$-12 \le h \le 12$, $-14 \le k \le 14$, $-14 \le l \le 14$	$-10 \le h \le 10$, $-12 \le k \le 12$, $-13 \le l \le 13$	$-12 \le h \le 12$, $-14 \le k \le 14$, $-17 \le l \le 17$
Measured reflections / independent	18628 / 4716	10609 / 2973	20850 / 5863
Absorption correction	numerical [24]	numerical [24]	numerical [24]
Max. / min. transmission	0.320 / 0.169	0.116 / 0.032	0.157 / 0.065
Structure solution	Direct Methods [25]	Direct Methods [25]	Direct Methods [25]
Structure refinement	full-matrix least-squares on F^2 [26]	full-matrix least-squares on F^2 [26]	full-matrix least-squares on F^2 [26]
Data/ ref. parameters	4716 / 83	2973 / 134	5863 / 167
$R1$ / $wR2$ [$I \ge 2\,\sigma(I)$]	0.044 / 0.108	0.038 / 0.058	0.057 / 0.111
$R1$ / $wR2$ (all data)	0.060 / 0.113	0.0525 / 0.060	0.089 / 0.120
Goodness-of-fit on F^2	1.18	1.20	1.01
Final Fourier residuals, e Å^{-3}	3.12 / −3.45	1.27 / −1.33	4.15 / −3.05

dral single crystals were observed, which cleave layer-wise. The yield was about 90 %.

$Pr_{10}(C_2)_2Br_{15}$: Silvery crystals were obtained by annealing Pr : $PrBr_3$: C in a molar ratio of 5 : 5 : 4 at 835 °C (24 d) with a yield of about 80 %.

$Pr_{14}(C_2)_3Br_{20}$: Black crystals with metallic luster, cleaving layer-wise, were obtained after annealing a mixture of Pr : $PrBr_3$: C in a molar ratio of 11 : 10 : 9 at 850 °C for 23 days with a yield of about 80 %.

In all cases $Pr_4C_xBr_5$ and/or $Pr_4(C_2)_{1-x}Br_5$ [13], respectively, were formed as by-products. In other syntheses, $Pr_6(C_2)Br_{10}$ and $Pr_{10}(C_2)_2Br_{15}$ were coexisting, but in no case together with $Pr_{14}(C_2)_3Br_{20}$.

Electron microscopy

HRTEM and SAED (selected area electron diffraction) were performed with a Philips CM30 ST microscope (300 kV, LaB_6 cathode, C_S = 1.15 mm). All manipulations for the preparation and transfer of the samples were carried out under dry Ar with the aid of a special device [18, 19]. A perforated carbon/copper net served as support for the crystallites. Simulations of HRTEM images (multislice formalism) and of SAED patterns (kinematical approximation) were calculated with the EMS program package [20] (spread of defocus: 70 Å, illumination semiangle: 1.2 mrad). All images were recorded with a Gatan Multiscan CCD camera and evaluated (including Fourier filtering) with the program DIGITAL MICROGRAPH 3.6.1 (Gatan). All HRTEM images were filtered after Fourier transformation by using a suitable band-pass mask.

X-Ray structure investigation

The reaction products were ground to fine powders under Ar atmosphere and sealed in glass capillaries for phase identification by a modified Guinier technique [21] (Cu$K_{\alpha 1}$: λ = 1.54056 Å; internal standard Si with a = 5.43035 Å; Fujifilm BAS-5000 image plate system). Single crystals were transferred to glass capillaries under Na-dried petroleum and sealed under Ar atmosphere. They were first examined by

Table 2. Atomic coordinates and displacement parameters (in Å^2). U_{eq} is defined as one third of the trace of the orthogonalized U_{ij} tensor.

Atom	*x/a*	*y/b*	*z/c*	U_{eq}
$Pr_6(C_2)Br_{10}$				
Pr1	0.1138(1)	0.0434(1)	−0.2336(1)	0.0095(1)
Pr2	−0.0258(1)	0.2853(1)	0.0852(1)	0.0107(1)
Pr3	0.3973(1)	0.1598(1)	0.2078(1)	0.0118(1)
Br1	0.2590(1)	0.0867(1)	0.4720(1)	0.0234(2)
Br2	0.5459(1)	0.1820(1)	−0.0858(1)	0.0143(1)
Br3	0.1742(1)	−0.2767(1)	−0.3675(1)	0.0146(1)
Br4	0.0925(1)	0.3750(1)	−0.1800(1)	0.0235(2)
Br5	0.3590(1)	0.4817(1)	0.2863(1)	0.0257(2)
C1	0.0963(9)	0.0353(7)	0.0483(7)	0.010(1)
$Pr_{10}(C_2)_2Br_{15}$				
Pr1	0.0804(1)	0.1797(1)	0.8849(1)	0.0140(1)
Pr2	0.0277(1)	0.1028(1)	0.2659(1)	0.0120(1)
Pr3	0.2472(1)	0.5402(1)	0.6408(1)	0.0136(1)
Pr4	0.1713(1)	0.4301(1)	0.0457(1)	0.0110(1)
Pr5	0.3357(1)	−0.2479(1)	0.8306(1)	0.0117(1)
Br1	0.3906(1)	0.2708(1)	0.8151(1)	0.0184(2)
Br2	0.2354(1)	−0.0926(1)	0.0621(1)	0.0184(2)
Br3	−0.0557(1)	0.4434(1)	0.7003(1)	0.0187(2)
Br4	0.4486(1)	0.3685(1)	0.4155(1)	0.0251(3)
Br5	0.3385(1)	0.1653(1)	0.2226(1)	0.0233(3)
Br6	0.2606(1)	0.0301(1)	0.6411(1)	0.0172(2)
Br7	0.1346(2)	−0.1851(1)	0.4635(1)	0.0253(3)
Br8	1/2	1/2	0	0.0288(4)
C1	−0.0435(12)	0.2959(11)	0.0600(11)	0.014(2)
C2	−0.1216(12)	0.3591(10)	0.1742(11)	0.012(2)
$Pr_{14}(C_2)_3Br_{20}$				
Pr1	0.4065(1)	0.2180(1)	0.5784(1)	0.0104(2)
Pr2	0.0585(1)	0.3820(1)	0.8208(1)	0.0101(2)
Pr3	0.3137(1)	0.4516(1)	0.9211(1)	0.0096(2)
Pr4	−0.0721(1)	0.7586(1)	0.8993(1)	0.0131(2)
Pr5	0.6990(1)	0.4145(1)	0.3612(1)	0.0137(2)
Pr6	0.3193(1)	0.7090(1)	0.3113(1)	0.0105(2)
Pr7	0.5322(1)	−0.0617(1)	0.1686(1)	0.0128(2)
Br1	0.3300(2)	0.4546(1)	0.4347(1)	0.0168(3)
Br2	−0.0627(2)	0.6373(2)	0.7020(1)	0.0186(3)
Br3	0.0543(2)	0.2523(2)	0.6251(1)	0.0248(4)
Br4	0.2855(2)	0.7228(1)	0.8300(1)	0.0180(3)
Br5	−0.3180(2)	0.4207(2)	0.8781(1)	0.0256(3)
Br6	0.4440(2)	0.1898(2)	0.0356(1)	0.0162(3)
Br7	0.4778(3)	0.0681(2)	0.3669(1)	0.0259(4)
Br8	0.1078(2)	0.1018(2)	0.9059(1)	0.0183(3)
Br9	−0.1767(2)	0.0230(2)	0.7760(2)	0.0248(3)
Br10	0.7735(2)	0.1544(1)	0.4815(1)	0.0159(3)
C1	0.3944(15)	0.2701(12)	0.7672(9)	0.008(2)
C2	0.0202(17)	0.4374(13)	0.0222(10)	0.013(2)
C3	0.3576(14)	0.3914(11)	0.7214(9)	0.005(2)

precession techniques before being characterized on a Stoe IPDS image plate instrument.

All three compounds crystallize in space group $P\bar{1}$ with Z = 1. Cell parameters and parameters for data collection and refinement are summarized in Table 1. Tables 2 and 3 contain the atomic coordinates and short distances in the three crystal structures.

Table 3. Shortest distances (Å), calculated on the basis of the X-ray single crystal investigation.

$Pr_6(C_2)Br_{10}$								
Pr1	Pr2	3.510(1)		Br2	3.133(1)			
	Pr2	3.561(1)		Br3	2.944(1)			
	Pr3	3.863(1)		Br4	2.940(1)			
	Pr3	3.931(2)		Br4	3.108(1)			
	Br1	3.114(1)		Br5	2.926(2)			
	Br1	2.982(2)		C1	2.609(6)			
	Br2	3.085(1)		C1	2.611(6)			
	Br3	2.941(1)	Pr3	Br1	2.925(1)			
	Br4	2.923(1)		Br2	3.067(1)			
	C1	2.588(6)		Br2	3.095(1)			
	C1	2.598(6)		Br3	3.094(1)			
Pr2	Pr3	3.826(1)		Br5	2.864(1)			
	Pr3	3.988(2)		C1	2.277(6)			
			C1	C1	1.44(1)			
$Pr_{10}(C_2)_2Br_{15}$								
Pr1	Pr1	4.014(2)		Br6	2.996(2)		Br1	3.090(2)
	Pr2	3.840(1)		Br7	3.002(2)		Br3	3.109(2)
	Pr4	3.973(1)		Br7	3.119(2)		Br5	3.077(2)
	Pr4	4.015(2)		C1	2.593(9)		Br8	3.105(9)
	Pr5	3.845(2)		C2	2.574(9)		C1	2.655(9)
	Br1	2.984(2)	Pr3	Pr4	3.979(2)		C1	2.683(10)
	Br2	3.057(2)		Pr4	4.019(1)		C2	2.677(10)
	Br2	3.069(2)		Pr5	3.882(1)		C2	2.713(9)
	Br3	2.996(2)		Br1	2.994(2)	Pr5	Br2	3.103(2)
	Br6	3.114(2)		Br3	2.980(2)		Br4	3.002(2)
	C1	2.29(1)		Br4	2.971(2)		Br5	3.120(1)
Pr2	Pr3	3.856(2)		Br4	3.105(2)		Br6	2.943(2)
	Pr4	3.669(2)		Br7	2.943(2)		Br8	2.957(1)
	Pr5	3.576(1)		C2	2.29(1)		C1	2.58(1)
	Br2	3.099(2)	Pr4	Pr4	3.375(1)		C2	2.574(9)
	Br5	2.918(1)		Pr5	3.692(2)	C1	C2	1.42(1)
$Pr_{14}(C_2)_3Br_{20}$								
Pr1	Pr2	3.718(2)		Br4	3.076(2)		Br4	2.985(2)
	Pr5	3.828(2)		Br5	3.092(2)		Br10	3.110(2)
	Pr6	3.587(1)		Br5	3.120(2)		C3	2.27(1)
	Pr7	3.778(2)		Br6	3.128(2)	Pr6	Pr1	3.587(1)
	Br1	3.098(2)		C1	2.68(1)		Pr3	3.701(2)
	Br3	2.932(2)		C2	2.66(1)		Pr7	3.822(2)
	Br7	3.001(2)		C2	2.66(1)		Br1	3.123(2)
	Br7	3.123(2)		C3	2.66(1)		Br3	3.089(2)
	Br10	2.988(2)	Pr4	Pr2	3.966(2)		Br5	2.984(2)
	C1	2.58(1)		Pr3	3.998(2)		Br9	3.016(2)
	C3	2.60(1)		Pr5	3.986(2)		Br10	2.959(2)
Pr2	Pr3	3.328(1)		Br2	2.990(2)		C1	2.58(1)
	Pr3	3.949(2)		Br4	2.958(2)		C3	2.59(1)
	Pr4	3.930(2)		Br6	3.038(2)	Pr7	Pr1	3.778(2)
	Br2	3.094(2)		Br8	2.971(2)		Pr2	4.009(2)
	Br3	3.070(2)		Br9	3.184(2)		Pr3	4.068(2)
	Br5	3.120(2)		C2	2.26(1)		Pr6	3.822(2)
	Br8	3.108(2)	Pr5	Pr1	3.828(2)		Br6	3.057(2)
	C1	2.67(1)		Pr2	3.951(2)		Br6	3.138(2)
	C2	2.69(1)		Pr3	3.971(1)		Br7	2.903(2)
	C2	2.71(1)		Pr4	3.986(2)		Br8	2.966(2)
	C3	2.67(1)		Pr6	3.877(2)		Br9	2.938(2)
Pr3	Pr2	3.949(2)		Br1	3.042(2)		C1	2.30(1)
	Pr4	3.850(2)		Br1	3.055(2)	C1	C3	1.38(2)
	Pr6	3.701(2)		Br2	2.968(2)	C2	C2	1.41(3)

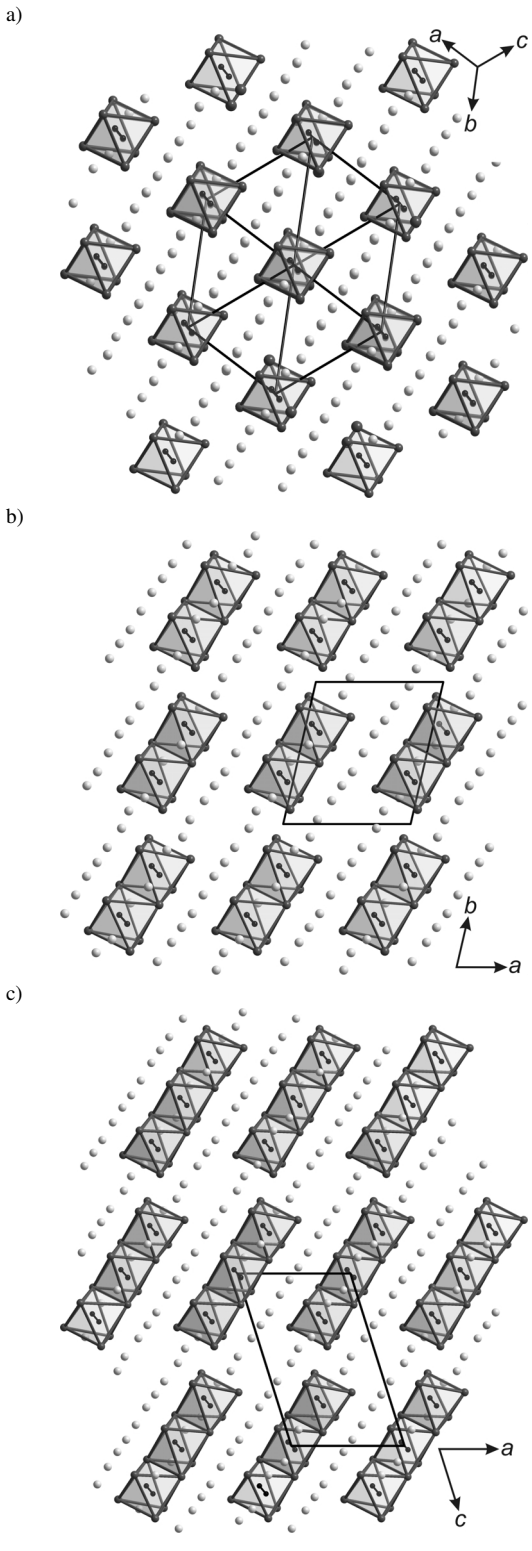

⟵ Fig. 1. Projections of the crystal structures of a) $Pr_6(C_2)Br_{10}$ along *ca*. [111], b) $Pr_{10}(C_2)_2Br_{15}$ along [001] and c) $Pr_{14}(C_2)_3Br_{20}$ along [010]. The Br, Pr and C atoms are illustrated as bright, grey and black spheres, respectively. Pr_6 clusters as well as the cell edges are emphasized with their contours.

Further details of the crystal structure investigations may be obtained from Fachinformationszentrum Karlsruhe, 76344 Eggenstein-Leopoldshafen, Germany (fax: +49-7247-808-666; e-mail: crysdata@fiz-karlsruhe.de, http://www.fiz-informationsdienste.de/en/DB/icsd/depot_anforderung.html) on quoting the deposition numbers CSD-420331 ($Pr_6(C_2)Br_{10}$), CSD-420332 ($Pr_{10}(C_2)_2Br_{15}$), and CSD-420333 ($Pr_{14}(C_2)_3Br_{20}$).

Results

Within the homologous series $Ln_{4n+2}(C_2)_nX_{5n+5}$ the compounds presented here comply with the first three members, n = 1, 2 and 3. The standard setting of the unit cell according to the lengths of the axes is chosen, but in order to reach a better comparison, the standard setting of $Pr_6(C_2)Br_{10}$ is changed *via* the matrix (–1 –1 0 0 –1 0 0 0 1) resulting in a = 7.571(2), b = 10.009(2), c = 9.062(2) Å, α = 67.13(3), β = 82.23(3), γ = 59.72(3)°.

One axis then becomes almost exactly 10 Å long, whereas it is approx. 10.9 Å for the other two compounds. One of the angles, 67°, as well as one of the axes, 9.05 – 9.09 Å, is nearly identical in all three compounds. Another axes is increased by approx. 2.5 Å per additional octahedron in the cluster. The partly different changes in the lattice parameters are caused by the fact that the octahedra do not lie parallel to one axis but in skewed positions in the cell. Nevertheless, some relationships in the parameters are obvious concerning common axes and similar angles.

The crystal structures of the three compounds may be depicted as an arrangement of shifted cluster rows, whose sections consist of single or condensed double- and triple-octahedra, respectively. In Figs. 1a – c these structures are shown as projections along the axes of approx. 10.9 and 10.0 Å, respectively, that relate to different directions. The Br atoms are aligned in diagonal rows, interrupted by C_2 dumbbells in perpendicular orientation to these rows. These C_2 units are each surrounded by Ln_6 octahedra. The latter are arranged in alternating layers according to an A, B stacking, *cf.* Figs. 2a – c.

The coordination of the Pr atoms by bridging Br atoms is equal to that of the corre-

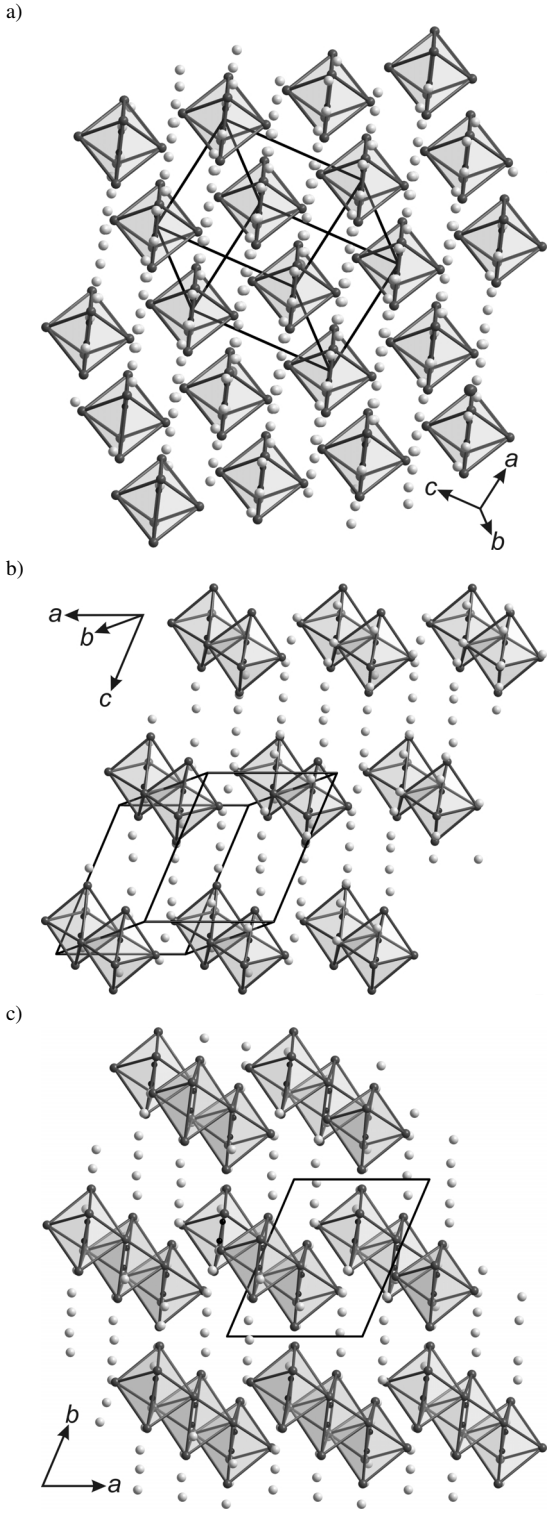

⟵ Fig. 2. Projections of the crystal structures of a) $Pr_6(C_2)Br_{10}$ along [121], b) $Pr_{10}(C_2)_2Br_{15}$ along *ca.* [6 −10 3] and c) $Pr_{14}(C_2)_3Br_{20}$ along [001]. The Br, Pr and C atoms are illustrated as bright, grey and black spheres, respectively. Pr_6 clusters as well as the cell edges are emphasized with their contours.

sponding La-I compounds and is further explained in ref. [7].

Distances between Pr atoms lie in the range from 3.33 to 4.07 Å. The shortest ones are observed in the waist, the connecting edge of the octahedra, and the longest are those from the vertices to the waist. In contrast to the reduced oxomolybdates containing empty and discrete cluster anions $[Mo_{4n+2}O_{6n+4}]^{(n+3)-}$ with only minor variations of the Mo–Mo distances [22], the repulsion between the highly charged interstitial C_2^{6-} ions leads to a significant distortion of the Ln_6 octahedra, which has frequently been described earlier, *e. g.* for the isostructural iodides. Additionally, the residual valence electrons which are localized in the common edge [23] enforce this effect. For $Pr_6(C_2)Br_{10}$, with only isolated octahedra, the distances vary only between 3.51 and 3.99 Å. Pr–Br distances range from 2.86 to 3.18 Å for all three compounds. The C–C bond lengths with 1.39 to 1.44 Å lie between those of usual C–C single and double bonds (*cf.* Table 3).

Electron microscopy

The electron microscopic investigation was performed on a heterogeneous sample composed of $Pr_{10}(C_2)_2Br_{16}$ and $Pr_6(C_2)Br_{10}$ with a ratio of *ca.* 60 : 40. The polyhedral crystals lay in different orientations on the copper grid, thus images of multiple directions were recorded. A selection of suitable SAED patterns is shown and discussed in the Addendum (below).

Due to the rapid amorphization of the crystals caused by beam damage, HRTEM images could only be taken along the [210] direction. These images, including the simulation for two focus values, are presented in Fig. 3. For comparison, the crystal potential, calculated on the basis of the X-ray model, as well as the HRTEM simulation for the Scherzer focus (Δf = −60 nm), are shown. In the potential representation large dark spots represent the metal atoms in the structure, and smaller ones the Br atoms. The resulting single octahedra are depicted with their contours. In the HRTEM simulation at Scherzer focus one could detect grey and bright areas within the black background.

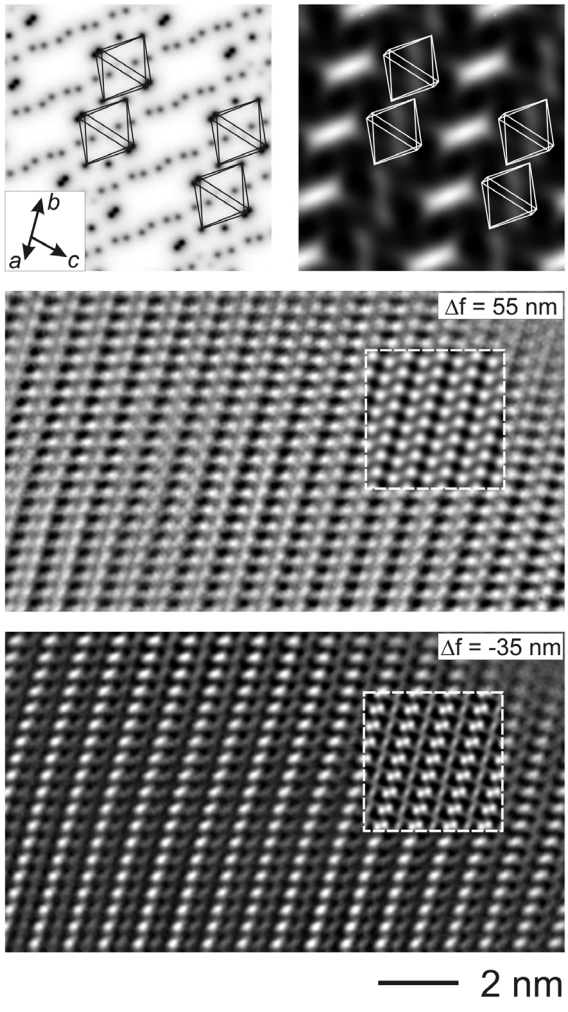

Fig. 3. Representation of crystal potential (left) and simulated HRTEM image (right, $\Delta f = -60$ nm, $t = 4.6$ nm) for $Pr_6(C_2)Br_{10}$ projected along [210] with the embedded cluster contours. Experimental images with inserted simulations (mid $\Delta f = 55$ nm, bottom $\Delta f = -35$ nm, $t = 4.6$ nm).

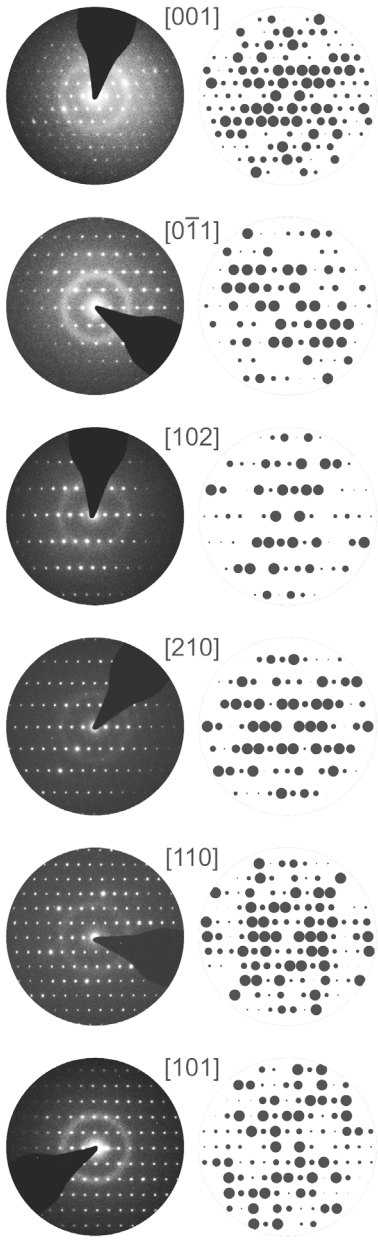

Fig. 4. Experimental SAED patterns (left) compared with the simulations (right) for six different directions of $Pr_6(C_2)Br_{10}$.

The dark contrasts corresponding with high values of the projected potential can be assigned to the Pr_6 octahedra. Residual dark contrasts that are forming rows can be assigned to the Br atoms. There, bright contrasts correlate with low values of the potential, *i. e.* with the voids between the octahedra and the rows of Br atoms.

The comparison of the simulation and the experimental high-resolution images in the lower part of Fig. 3 shows a good agreement of the contrasts. At $\Delta f = 55$ nm the contrasts are completely inverted, but agree also with the embedded simulation. With the knowledge of the structural relation to the image, one could easily comprehend the diagonal arrangement of the single octahedra represented by strings of white spots at this focus value, which correlate with the corners of the octahedra. Accordingly, the dark spots represent the cores of the octahedra. For $\Delta f = -35$ nm a contrast reversal occurs, and the dark spots now correspond with the heavy atoms and are interpreted as the corners of the octahedra.

Addendum

Beside the [001] axes, in Fig. 4 some diagonal directions are also depicted, whose SAED patterns all show clear bright spots without any diffuse or elongated reflections. Due to multiple scattering, the observed intensities partly disagree with the simulations on the right, which are calculated on the basis of the model derived from the X-ray data. Beside the obvious inversion symmetry, no further symmetry elements are observed. In some orientations additional spots occur belonging to higher order Laue zones.

Acknowledgement

The authors are indebted to Dr. C. Hoch and H. Gärttling for single crystal X-ray investigations.

[1] H. Schäfer, H. G. Schnering, *Angew. Chem.* **1964**, *76*, 833.
[2] A. Simon, *Angew. Chem.* **1981**, *93*, 23; *Angew. Chem., Int. Ed. Engl.* **1981**, *20*, 1.
[3] A. Simon, *Angew. Chem.* **1988**, *100*, 163; *Angew. Chem., Int. Ed. Engl.* **1988**, *27*, 159.
[4] A. Simon, Hj. Mattausch, G. J. Miller, W. Bauhofer, R. K. Kremer, *Handbook on the Physics and Chemistry of Rare Earth*, Vol. 15, Elsevier Science Publ., Amsterdam **1991**, p. 191.
[5] J. D. Corbett, *J. Chem. Soc., Dalton Trans.* **1996**, *12*, 575.
[6] G. Meyer, *Chem. Rev.* **1988**, *88*, 93.
[7] Hj. Mattausch, A. Simon, L. Kienle, C. Hoch, C. Zheng, R. K. Kremer, *Z. Anorg. Allg. Chem.* **2006**, *632*, 1661.
[8] Hj. Mattausch, C. Hoch, A. Simon, *Z. Anorg. Allg. Chem.* **2005**, *631*, 1423.
[9] M. C. Schaloske, A. Simon, unpublished results.
[10] L. Kienle, Hj. Mattausch, A. Simon, *Angew. Chem.* **2006**, *118*, 8204; *Angew. Chem. Int. Ed.* **2006**, *45*, 8036.
[11] R. Wiglusz, I. Pantenburg, G. Meyer, *Z. Kristallogr. NCS* **2007**, *222*, 9.
[12] L. Kienle, M. C. Schaloske, Hj. Mattausch, V. Duppel, A. Simon, *Solid State Sci.* **2008**, *10*, 401.
[13] Hj. Mattausch, M. C. Schaloske, C. Hoch, C. Zheng, A. Simon, *Z. Anorg. Allg. Chem.* **2008**, *634*, 491.
[14] Hj. Mattausch, E. Warkentin, O. Oeckler, A. Simon, *Z. Anorg. Allg. Chem.* **2000**, *626*, 2117.
[15] M. C. Schaloske, Hj. Mattausch, L. Kienle, A. Simon, *Z. Anorg. Allg. Chem.* **2008**, *634*, 2246.
[16] A. Simon, E. Warkentin, R. Masse, *Angew. Chem.* **1981**, *93*, 1071; *Angew. Chem., Int. Ed. Engl.* **1981**, *20*, 1013.
[17] G. Meyer, P. Ax, *Mater. Res. Bull.* **1982**, *17*, 1447.
[18] P. Jeitschko, A. Simon, R. Ramlau, Hj. Mattausch, *Europ. Microscopy Microanal.* **1997**, *46*, 21.
[19] P. Jeitschko, A. Simon, R. Ramlau, Hj. Mattausch, *Z. Anorg. Allg. Chem.* **1997**, *623*, 1447.
[20] P. A. Stadelmann, *Ultramicroscopy* **1987**, *21*, 131.
[21] A. Simon, *J. Appl. Crystallogr.* **1970**, *3*, 11.
[22] Hj. Mattausch, A. Simon, E.-M. Peters, *Inorg. Chem.* **1986**, *25*, 3428.
[23] S. Satpathy, O. K. Andersen, *Inorg. Chem.* **1985**, *24*, 2604.
[24] X-RED32 (version 1.26), X-SHAPE2 (version 2.05), Crystal Optimisation for Numerical Absorption Correction, Stoe & Cie. GmbH, Darmstadt (Germany) **2004**.
[25] G. M. Sheldrick, SHELXS-97, Program for the Solution of Crystal Structures, University of Göttingen, Göttingen (Germany) **1997**.
[26] G. M. Sheldrick, SHELXL-97, Program for the Refinement of Crystal Structures, University of Göttingen, Göttingen (Germany) **1997**. See also: G. M. Sheldrick, *Acta Crystallogr.* **2008**, *A64*, 112.